The American Journal of Pathology, Vol. 171, No. 3, September 2007

DOI: 10.2353/ajpath.2007.070056

Cardiovascular, Pulmonary and Renal Pathology

A Thrombospondin-1 Antagonist of Transforming Growth Factor-β Activation Blocks Cardiomyopathy in Rats with Diabetes and Elevated Angiotensin II

Souad Belmadani,* Juan Bernal,* Chih-Chang Wei,† Manuel A. Pallero,‡ Louis Dell'Italia,† Joanne E. Murphy-Ullrich,‡ and Kathleen H. Berecek*

From the Department of Physiology and Biophysics, the Department of Pathology and the BioMatrix Engineering and Regenerative Medicine Center,‡ and Department of Medicine,† Division of Cardiovascular Medicine, Center for Heart Failure Research, University of Alabama at Birmingham, Birmingham, Alabama*

In diabetes and hypertension, the induction of increased transforming growth factor-β (TGF-β) activity due to glucose and angiotensin II is a significant factor in the development of fibrosis and organ failure. We showed previously that glucose and angiotensin II induce the latent TGF-β activator thrombospondin-1 (TSP1). Because activation of latent TGF-β is a major means of regulating TGF-β, we addressed the role of TSP1-mediated TGF-β activation in the development of diabetic cardiomyopathy exacerbated by abdominal aortic coarctation in a rat model of type 1 diabetes using a peptide antagonist of TSP1-dependent TGF-β activation. This surgical manipulation elevates initial blood pressure and angiotensin II. The hearts of these rats had increased TSP1, collagen, and TGF-β activity, and cardiac function was diminished. A peptide antagonist of TSP1-dependent TGF-β activation prevented progression of cardiac fibrosis and improved cardiac function by reducing TGF-β activity. These data suggest that TSP1 is a significant mediator of fibrotic complications of diabetes associated with stimulation of the renin-angiotensin system, and further studies to assess the blockade of TSP1-dependent TGF-β activation as a potential antifibrotic therapeutic strategy are warranted. ***(Am J Pathol 2007, 171:777–789; DOI: 10.2353/ajpath.2007.070056)***

Diabetic cardiomyopathy is a major cause of congestive heart failure in diabetics and can occur independently of atherosclerosis. This disease occurs more frequently in diabetics with accompanying hypertension, particularly in African Americans.[1,2] Interstitial fibrosis is a major factor underlying the myocardial hypertrophy and diastolic dysfunction that characterize diabetic cardiomyopathy.[1–4] The severity of fibrosis is increased in diabetic animals that also have hypertensive disease.[3,5] Both hyperglycemia and angiotensin II are critical in the pathogenesis of fibrosis.

Remodeling of the myocardium in diabetes affects both the cardiac myocyte and the cardiac fibroblast.[2,6] Alterations in the cardiac myocyte include hypertrophy and altered sarcomere organization. Cardiac fibroblasts exhibit increased proliferation and aberrant remodeling of the extracellular matrix with net accumulation of extracellular matrix in the interstitium and surrounding the coronary arteries. Cardiac fibrosis also contributes to left

Supported by National Institutes of Health grants HL50061 and DK60658 to J.E.M.-U., HL31515 to K.H.B., and by P50HL077100 to L.D. This investigation was conducted in a facility constructed with support from Research Facilities Improvement Program grant no. C06 RR 15490 from the National Center for Research Resources, National Institutes of Health. Funds for the purchase of the Applied Biosystems 4000 Qtrap came from a National Center for Research Resources Shared Instrumentation grant S10 RR19231. Operation of the Mass Spectrometry Shared Facility comes from funds provided by the University of Alabama Birmingham (UAB) Comprehensive Cancer Center Core Support grant (P30 CA13148), the Purdue-UAB Botanicals Center for Age-Related Disease (P50 AT00477), the UAB Center for Nutrient-Gene Interaction in Cancer Prevention (U54 CA100949), the UAB Skin Disease Research Center (P30 AR050948), and the UAB Polycystic Kidney Disease Center (P30 DK74038).

Accepted for publication May 23, 2007.

Supplemental material for this article can be found on *http://ajp.amjpathol.org*.

Current address of S.B.: Department of Physiology, LSU Health Sciences Center, New Orleans, Louisiana.

Current address of J.B.: Division of Cardiology, Wayne State University, Detroit, Michigan.

The authors state that there are no financial or other conflicts of interest.

Editorial note: A guest editor acted as editor-in-chief for this manuscript. No person at the University of Alabama at Birmingham was involved in the peer review process or final disposition for this article.

Address reprint requests to Joanne E. Murphy-Ullrich, Ph.D., Department of Pathology, University of Alabama at Birmingham, 668 Volker Hall, 1530 3rd Ave. South, Birmingham, AL 35294-0019. E-mail: murphy@uab.edu.

ventricular hypertrophy and is the major determinant of altered left ventricular compliance leading to systolic and diastolic dysfunction.[6,7]

The fibrogenic cytokine transforming growth factor (TGF-β) is known to play a significant role in fibrotic cardiac remodeling, and multiple factors altered in the diabetic condition, including glucose and angiotensin II, stimulate both increased TGF-β protein expression and increases in TGF-β bioactivity.[8–12,14] The cardiac renin-angiotensin system is up-regulated in diabetes and has been implicated in cardiac fibrosis.[6,7,15] Angiotensin II signaling through the AT_1 receptor results in cardiac fibroblast proliferation and net accumulation of fibrillar collagen *in vitro* and cardiac fibrosis *in vivo*.[7] Angiotensin II mediates end-organ fibrosis, independent of hemodynamic effects, through stimulation of TGF-β.[9,11,16–18] Valsartan, an antagonist of the AT1 receptor, attenuates myocardial interstitial fibrosis in diabetic rats by decreasing expression of active TGF-β in the heart.[13] TGF-β1-neutralizing antibodies and other TGF-β antagonists such as tranilast reduce cardiac and renal fibrosis in both hypertensive and diabetic animal models.[13,19–21] In addition, another AT1 receptor antagonist, losartan, prevents vascular remodeling, leading to aortic aneurysm in a mouse model of Marfan's syndrome by reducing levels of active TGF-β.[22]

The potent fibrogenic action of TGF-β is regulated at multiple levels, including protein expression and secretion, localization to the extracellular matrix, and modulation of receptor and signaling pathways.[23,24] TGF-β is secreted as a latent complex that must be activated to elicit fibrogenic effects. Activation of the latent complex is a key means of regulation of latent TGF-β activity.[25,26] Several factors can activate latent TGF-β, including proteases, integrins, latent TGF-β-binding protein, oxidant modification of the latent complex, and the matricellular protein thrombospondin-1 (TSP1).[25–30] TSP1 binds to the latent TGF-β complex through defined sequences in both the latency-associated peptide and in the mature domain.[31–34] TSP1 binding to the latent complex induces a conformational change in the latent TGF-β complex, rendering it biologically active.[25] We identified a conserved sequence (LSKL) in the latency-associated peptide that is necessary for latency and that is recognized by the activating sequence of TSP1.[31] A peptide mimetic of this sequence prevents TSP1 binding to the latent complex and acts as an antagonist of TSP1-mediated TGF-β activation.[31,35]

TSP1 levels are increased in the hearts of animals with diabetic cardiomyopathy.[36] Previous studies from our lab and others showed that both glucose and angiotensin II stimulate increased TSP1 expression, resulting in enhanced TGF-β activation.[37–40] Glucose stimulation increases TSP1 through enhancing USF2-dependent transcription via protein kinase C, extracellular signal-regulated kinase, and p38 mitogen activated protein kinase (MAPK) pathways to overcome nitric oxide-protein kinase G-mediated transcriptional repression.[41] Angiotensin II induces TSP1 production in human mesangial cells via p38 MAPK and c-Jun NH_2-terminal kinase.[39]

In these current studies, we tested the hypothesis that TSP1, through control of TGF-β activation, is a major mediator of the myocardial complications of diabetes with activation of the renin-angiotensin system. We used a peptide antagonist of TSP1, LSKL, to selectively block glucose and angiotensin II-stimulated increases in TGF-β activity as a therapeutic strategy to modify fibrotic disease progression in a rat model of type 1 diabetes with activation of the renin-angiotensin system by surgical manipulation. The peptide antagonist of TSP1-dependent TGF-β activation reduced cardiac fibrosis, myocyte hypertrophy, and improved left ventricular function in these animals. These data support the hypothesis that TSP1 is a key mediator of fibrogenic changes induced by diabetes and suggest that blockade of TSP1-dependent TGF-β activation represents a novel therapeutic strategy to prevent or reverse fibrosis.

Materials and Methods

Peptides

Both peptides (LSKL and LSAL) were purchased from AnaSpec, Inc., San Jose, CA. Peptides were purified by reversed phase high-performance liquid chromatography and determined to be >98% pure by mass spectrometry.

Animal Model

Male Wistar Kyoto rats, 250 to 300 g, were used for all studies (Charles River, Wilmington, MA). Animals were maintained and handled in accordance with approved Institutional Animal Care and Use Committee standards. In experimental animals, hypertension was induced by abdominal aortic coarctation, and diabetes was induced by a single injection of streptozotocin (STZ). Rats were anesthetized by intraperitoneal administration with ketamine (80 to 100 mg/kg) plus xylazine (5 mg/kg). Under sterile conditions, the abdominal cavity was opened via a midline incision, and the abdominal aorta and both renal arteries were exposed. Partial constriction of the abdominal aorta between the renal arteries was made using a small Hemoclip (Weck, Research Triangle Park, NC) set to an internal diameter of 0.45 mm. One week after recovery from surgery, animals were given a single intraperitoneal injection of STZ (52 mg/kg) (Sigma, St. Louis, MO) dissolved in citric acid buffer, pH 4.6. Sham animals underwent the same surgical procedure without placement of the clip and received an injection of citric acid buffer without STZ. Injected animals were fasted for 12 hours, and blood glucose was measured 1 week after injection. Blood glucose measurements were obtained from tail vein samples using a blood glucose meter (Prestige Smart System HDI; Home Diagnostics, Inc., Fort Lauderdale, FL). Glucose levels in the urine were determined with glucose reagent strips (Keto-Diastix; Bayer, Elkhart, IN). Indirect systolic blood pressure was determined by tail-cuff plethysmography in conscious, restrained rats.[42] Animals were sacrificed 12 weeks after surgery.

Peptide Administration

Experimental and sham animals were randomly placed into the following groups: Sham, Sham + LSKL, Sham + LSAL, diabetic with abdominal aortic coarctation (DAAC), DAAC + LSKL, and DAAC + LSAL (five to eight animals per group). Peptide administration began 6 weeks following induction of experimental or sham procedures. The peptides were solubilized in sterile saline and given to animals by intraperitoneal injection at a dose of 4 mg/kg, three times per week for 6 weeks.

Hemodynamic and Echocardiographic Measurements

Mean arterial pressure was measured in anesthetized animals (ketamine/xylazine, 80:10 mg/kg) using an intravascular pressure transducer (model SPR-294A Millar Micro-Tip catheter transducer; Millar Instruments, Houston, TX) introduced into the aorta via the right carotid artery. Once pressure measurements were completed, echocardiography was performed in the rats using a 15-MHz transducer attached to an Agilent Sonos 5500 echocardiography machine. M-mode measurement was used to determine left ventricular end-diastolic dimension (LVEDD), left ventricular end-systolic dimension (LVESD), and posterior wall thickness (PW).[43] Doppler tracings of left ventricular outflow at the aortic valve level were obtained to determine ejection time (EjT) and the time of the R-R interval. Left ventricular systolic chamber function was assessed from the rate-corrected velocity of circumferential shortening (VCF_r), which was calculated using the equation: $(LVEDD - LVESD/LVEDD)/(EjT - RR^{0.5})$, where LVEDD is the left ventricular end-diastolic diameter, LVESD is the left ventricular end-systolic diameter, and RR is the time of the R-R interval.

Tissue Angiotensin II Assay

Cardiac angiotensin II peptide concentrations were determined by a method previously established that combines solid-phase extraction, high-performance liquid chromatography, and radioimmunoassay.[44,45] Radioimmunoassay of relevant peaks revealed detectable levels of angiotensin (Ang) II in all left ventricular (LV) samples examined. Antibodies to Ang II were raised in New Zealand White rabbits immunized against peptide conjugated to poly-L-lysine, as previously described.[44] The sensitivity of the radioimmunoassay for Ang II is 2 pg/ml. For each experimental group, 300 to 430 mg of cardiac tissue was assayed.

Collagen Measurement

Serial sections (5 μm) of formalin-fixed, paraffin-embedded tissues were stained with picric acid-Sirius red for quantification of collagen. Images of cross sections of the left ventricle were digitized using a ×10 or ×20 objective of an IMT-2 inverted microscope (Olympus, Tokyo, Japan) equipped with a SPOT digital camera (Diagnostic Instruments, Sterling Heights, MI). Images were analyzed using Image Pro Plus (Media Cybernetics, Silver Spring, MD). The percentage of the field area that stained for collagen was determined for 20 to 30 fields for each transmural region (subendomyocardial and subepicardial), and the mean value was calculated for each region.

Hydroxyproline Content

Total collagen content of the left ventricle was quantified biochemically by the hydroxyproline assay.[46] Specimens were dried and hydrolyzed in 12 N HCl at 120°C overnight. Hydrolysates were neutralized and mixed with chloramine T solution and oxidized for 20 minutes at room temperature. The oxidized product was reacted with *p*-dimethylaminobenzaldehyde in ethanol and H_2SO_4 solution at 60°C for 20 to 25 minutes, and the resulting chromophore was quantified spectrophotometrically at 557 nm against a standard curve of known hydroxyproline concentration (3 to 20 μg/ml).

Immunohistochemistry

Formalin-fixed hearts were embedded in paraffin and sectioned at 5 μm. Slides were heated at 58°C for 1 hour. After removal of paraffin, endogenous peroxidase activity was quenched by 5-minute incubation with 3% H_2O_2 in H_2O. Slides were placed in 0.01 mol/L glycine solution, pH 3, microwaved for 10 minutes, and cooled to room temperature. Slides were then placed in 0.5 mmol/L casein in phosphate-buffered saline, pH 7.4, for 30 minutes. Sections were incubated overnight at 4°C with mouse monoclonal antibody against TSP1 (mAb 133 at 10 μg/ml, purified by our lab in a joint effort with the University of Alabama at Birmingham Hybridoma Core facility).[30] For every section, a negative control without anti-TSP1 antibody was processed simultaneously. After three 5-minute washes in Tris-buffered saline (TBS)-T (10 mmol/L Tris-HCl, 0.15 mol/L NaCl, 8 mmol/L sodium azide, and 0.05% Tween 20, pH 8.0), a secondary biotinylated antibody was added for 45 minutes at room temperature. After three 5-minute washes in TBS-T, the avidin biotin-peroxidase complex (Vector Labs, Burlingame, CA) was applied for 30 minutes at room temperature. The color reaction was developed with the diaminobenzidine detection kit (Vector Labs) and counterstained with hematoxylin.

For detection of active TGF-β, sections were treated with hyaluronidase (Sigma Chemical Co., St. Louis, MO) at 1 mg/ml in 0.1 mol/L sodium acetate, pH 5.5, containing 0.85% NaCl at 37°C for 30 minutes. After blocking with 5% normal goat serum, a rabbit polyclonal antibody to active TGF-β (LC-1-30; a gift from Dr. Kathy Flanders, National Cancer Institute, Lab of Cell Regulation and Carcinogenesis, National Institutes of Health, Bethesda, MD)[47] was used in TBS containing 0.1% bovine serum albumin overnight at 4°C. Antibody LC-1-30 recognizes intracellular active TGF-β and has been used to detect active TGF-β in paraffin-embedded tissues.[48] Biotinylated goat-anti-rabbit IgG (Vector Labs) was added, followed by avidin peroxidase conjugate.

For immunostaining of phosphorylated Smad 2, sections were treated with sodium citrate buffer (10 mmol/L, pH 6.0) at 100°C for 10 minutes. After blocking with 5% bovine serum albumin in TBS, a rabbit polyclonal antibody anti-phosphorylated Smad 2 (Cell Signaling, Beverly, MA) was incubated with sections overnight at 4°C. Sections were washed and incubated with biotinylated goat-anti-rabbit IgG (Vector Labs) and then avidin peroxidase conjugate. Sections were counterstained with hematoxylin.

Staining was quantified by image analysis as described for collagen measurement. Ten to 15 fields from the left ventricle were captured, digitized, and analyzed. For TGF-β and TSP1, staining was quantified by dividing the sum area of the positively stained area by the sum of the reference area. Results are expressed as percent area positive for TGF-β or TSP1. For quantification of phosphorylated Smad 2, the number of positive (brown) nuclei in 10 to 15 fields in each of three separate sections of left ventricle was counted. Blue-staining nuclei were counted in the same fields. The percent Smad 2-positive nuclei (brown nuclei) was calculated as a percentage of the total nuclei [positive (brown) and negative (blue)].

Immunoblot Analysis

Immunoblot analysis was performed under reducing conditions as described previously.[49] Left ventricular tissues obtained from sham and DAAC animals were homogenized by sonication and lysis in buffer containing 0.1% Triton X-100. After centrifugation at 10,000 $\times$ *g* for 20 minutes at 4°C, the supernatant was analyzed for determination of Smad proteins and for TSP1. Total protein concentration of all samples was measured using the bicinchoninic acid method. Equal protein amounts were loaded and analyzed by immunoblotting on separate gels. Primary antibodies were diluted in TBS-T: rabbit anti-phosphorylated Smad 2 (1:4000) (Cell Signaling), mouse anti-total Smad 2 (1:500; Transduction Laboratories, San Diego, CA), and mouse anti-TSP1 (mAb 133, 10 μg/ml). The specific bands of target proteins were visualized by enhanced chemiluminescence according to the manufacturer's instructions (Amersham Life Science Inc. Arlington Heights, IL). Bands were quantified using Image Gauge (version 3.41) software (Fuji Photo Film; Tokyo, Japan). Equal loading of protein was confirmed by Coomassie staining of membranes and analysis of actin.

Detection of LSKL Peptide in Body Fluids by Liquid Chromatography-Mass Spectrometry

Sham and DAAC rats (8 to 10 weeks of age) were treated with a single dose (3 mg/kg) of LSKL peptide by intraperitoneal injection 6 weeks after experimental manipulation. Urine was collected for 24 hours, and serum was obtained at 4, 8, 24, 48, and 72 hours following injection of the peptide. Preliminary studies established that LSKL peptide could be detected by liquid chromatography-mass spectrometry when added to processed normal rat urine or serum over a concentration range of 50 nmol/L to 5 μmol/L.[50] Urine samples were processed by centrifugation at 2500 rpm for 5 minutes at 4°C to remove cell debris. Serum samples were fractionated using 5MWCO Amicon Ultra4 centrifugal filters (Millipore, Inc., Bedford, MA) with centrifugation for 10 minutes at 3000 rpm at 4°C to remove proteins >5000 d. Processed samples were further fractionated by reverse phase chromatography on a C18 column in Zip tips (Millipore) equilibrated in 0.1% trifluoroacetic acid. Samples (10 μl) were prepared to a final pH of 4 in 0.1% trifluoroacetic acid and added to the equilibrated Zip tips. Unbound material was washed with 0.1% trifluoroacetic acid. Bound proteins were eluted in a 5-μl volume in 0.1% trifluoroacetic acid + 50% acetonitrile. The final sample volume was raised to 25 μl by the addition of Milli-Q water (Millipore). The quantitative measurement of the LSKL peptide was performed using the triple quadrupole capabilities provided by the ABI Sciex 4000Q-trap mass spectrometer (Applied Biosystems, Foster City, CA), which is sensitive in the range of 1 to 10 fmol.

Statistical Analysis

Data (mean $\pm$ SEM) were analyzed using one-way analysis of variance followed by Student Newman-Keuls posthoc analysis for statistical comparisons between groups (InStat software; GraphPad Software Inc., San Diego, CA). A P value <0.05 was considered to be significant.

Results

Characterization of DAAC

Diabetes was confirmed in rats by detection of elevated blood glucose levels 7 to 10 days after injection of streptozotocin. All groups of animals receiving streptozotocin had significant elevations of blood glucose, water consumption, and reduced body weight compared with sham-treated animals (Table 1). Rats were also subjected to abdominal aortic coarctation, which is a well-established method of inducing hypertension.[3,51] At 3 weeks, the diabetic rats with abdominal aortic coarctation (DAAC) had elevated blood pressure as measured by the tail-cuff method[52] (Table 2). However, as the diabetic disease progressed, beginning at 5 to 6 weeks we observed a decrease of mean arterial pressure in the DAAC rats. These observations are consistent with other published studies, which show that streptozotocin produces a lowering of blood pressure in rats.[42,52] Furthermore, the decrease in blood pressure is consistent with a decrease in cardiac function as indicated by the abnormal echocardiographic parameters measured at 12 weeks (Table 2). Despite the lack of measurable elevations in blood pressure, the renin-angiotensin system was activated in these animals, because levels of angiotensin II peptide were elevated in the left ventricles of DAAC rats compared with sham control rats (Figure 1).

Myocardial Fibrosis Occurs in DAAC Animals

At both 6 and 12 weeks after disease induction, significant fibrotic changes were evident in the myocardium as evaluated by image analysis of picric acid-Sirius red-stained

Table 1. Characteristics of DAAC Rats at 12 Weeks

	Sham + saline	Sham + LSKL	Sham + LSAL	DAAC + saline	DAAC + LSKL	DAAC + LSAL
BW (g)	450 ± 27	405 ± 16	409 ± 28	251 ± 25*	254 ± 48*	265 ± 27*
Water intake (ml/day)	31 ± 2 (8)	34 ± 4 (8)	37 ± 3 (8)	114 ± 5* (5)	115 ± 6* (8)	122 ± 10* (5)
Blood glucose (mg/dl)	118 ± 5 (8)	136 ± 14 (8)	128 ± 8 (8)	309 ± 22* (5)	306 ± 14* (8)	314 ± 38* (5)
HW/BW	3.98 ± 0.1 (8)	3.93 ± 0.1 (8)	3.83 ± 0.07 (8)	4.57 ± 0.2* (5)	4.94 ± 0.52* (8)	4.72 ± 0.2* (5)
LV weight (g)	1.28 ± 0.11 (8)	1.18 ±0.08 (8)	1.18 ± 0.08 (8)	0.80 ± 0.04* (5)	0.84 ± 0.09* (8)	0.93 ± 0.25* (5)
LVW/BW	2.82 ± 0.1 (8)	2.89 ± 0.08 (8)	2.82 ± 0.04 (8)	3.42 ± 0.1* (5)	3.58 ± 0.3* (8)	3.42 ± 0.1* (5)
Myocyte area (μm)	1409 ± 173 (7)			3234 ± 543* (7)	1586 ± 206 (6)	3564 ± 130* (6)

Data are presented as means ± SEM. The number of animals analyzed per group is indicated in parentheses. BW, body weight (grams); HW/BW, heart weight-to-body weight ratio; LV weight, left ventricular weight (grams); LVW/BW, LV weight-to-heart weight ratio.
*$P < 0.001$ versus sham + saline calculated using one-way analysis of variance.

sections of the myocardium and by measurement of hydroxyproline content. Picric acid-Sirius red staining was increased in the left ventricular interstitium of DAAC rats compared with sham animals (Figure 2A). Increased left ventricular fibrosis was present in both endocardium and epicardium (Figure 2B). Hydroxyproline content in the left ventricle at 12 weeks was increased 2.4-fold in DAAC rats compared with sham animals (Figure 2C). Interstitial fibrosis was accompanied by myocyte hypertrophy (Table 1). Perivascular fibrosis is also observed in the DAAC rats (Figure 2A). Thus, this model replicates the hallmarks of diabetic cardiomyopathy, which include myocardial fibrosis and left ventricular diastolic dysfunction.[1–5]

TSP1 Is Increased in the Hearts of DAAC Animals

We examined whether TSP1 protein is up-regulated in the DAAC model. Immunoblot analysis of left ventricular lysates showed increased TSP1 levels in hearts of DAAC rats (Figure 3A). Immunohistochemical analysis of hearts from sham animals after 12 weeks of disease induction showed weak staining for TSP1 in cardiac myocytes (Figure 3B). TSP1 was primarily localized to the endocardium but only weak or absent in the epicardium of the left ventricular sections. In DAAC animals, TSP1 was markedly increased in the left ventricular myocardium compared with sham animals (Figure 3B). These data establish that TSP1 is elevated in myocardial tissues, which exhibit fibrotic complications because of diabetes and activation of the renin-angiotensin system.

TGF-β Activity Is Increased in the Hearts of DAAC Animals

Since there is no direct method for quantifying active TGF-β in tissues, we used three different approaches to determine relative levels of TGF-β activity. Relative levels of active TGF-β were assessed in the heart by immunohistochemical analyses of tissues stained with an antibody previously shown to recognize the active form of TGF-β in formalin-fixed tissues[47,48] and by staining for phosphorylated Smad 2 (Figure 4). In normal animals, staining for active TGF-β was localized primarily to the myocardium (Figure 4A), and phosphorylated Smad 2 staining was sparse to absent in the hearts of control sham animals (Figure 4B). At 12 weeks following disease induction, both active TGF-β and phosphorylated Smad 2 were increased in the hearts of DAAC animals compared with sham animals (Figure 4, A and B). In tissues from DAAC animals, phosphorylated Smad 2 was observed in the nuclei of both cardiac myocytes and interstitial fibro-

Table 2. Evaluation of Cardiac Function

	Sham + saline	S + LSKL	S + LSAL	DAAC + saline	DAAC + LSKL	DAAC + LSAL
MAP at 3 weeks (mmHg)	120 ± 5 (3)	115 ± 4 (3)	118 ± 4 (3)	145 ± 4* (3)	155 ± 6* (3)	148 ± 4* (3)
MAP at 12 weeks (mmHg)	112 ± 7	111 ± 3	106 ± 5	96 ± 4	112 ± 5	90 ± 3
PW (mm)	1.48 ± 0.02	1.44 ± 0.05	1.50 ± 0.15	1.39 ± 0.12	1.47 ± 0.04	1.42 ± 0.10
LVEDD (mm)	7.61 ± 0.05	7.48 ± 0.11	7.80 ± 0.26	7.96 ± 0.07*	7.37 ± 0.24†	7.93 ± 0.08*
LVEDD/PW	5.13 ± 0.01	5.22 ± 0.13	5.49 ± 0.41	6.11 ± 0.24‡	5.01 ± 0.15§	6.07 ± 0.38‡
LVESD (mm)	3.97 ± 0.10	4.14 ± 0.40	4.10 ± 0.45	4.56 ± 0.12*	3.89 ± 0.15†	4.11 ± 0.11
VCFr	5.9 ± 0.2	5.4 ± 0.5	5.3 ± 0.2	3.8 ± 0.2*	4.7 ± 0.3†	4.0 ± 0.7*

Measurements were made at 12 weeks after disease induction, which is 6 weeks after initiation of peptide treatment. Data are expressed as the mean ± SEM. For the blood pressure measurement at 3 weeks, three animals were measured from each group. For the others parameters (MAP at 12 weeks, PW, LVEDD, LVESD, VCFr, and LVEDD/PW), eight animals were evaluated in the sham, sham + LSKL, sham + LSAL, and DAAC + LSKL groups. Five animals were evaluated in the DAAC + saline and in the DAAC + LSAL groups. MAP, mean arterial pressure; PW, posterior wall thickness; LVEDD, left ventricular end-diastolic dimension; LVESD, left ventricular end-systolic dimension; VCFr, rate-corrected velocity of circumferential shortening; LVEDD/PW, left ventricular end-diastolic dimension/posterior wall thickness ratio.
*$P < 0.05$ versus the sham + saline group.
†$P < 0.05$ versus DAAC + saline group as calculated by one-way analysis of variance.
‡$P < 0.01$ versus sham + saline group.
§$P < 0.01$ versus DAAC + saline group as calculated by one-way analysis of variance.

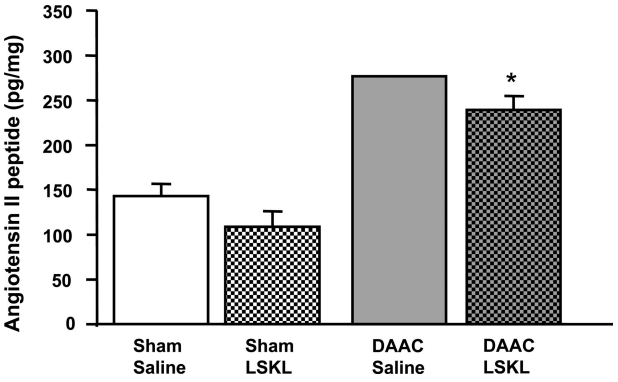

Figure 1. Angiotensin II peptide is increased in the hearts of DAAC rats. Levels of angiotensin II (ANG II) peptide were measured in tissues from the left ventricles of sham and DAAC rats treated with either saline or LSKL peptide. Sham + saline ($n = 6$), Sham + LSKL ($n = 6$), DAAC + saline ($n = 2$), and DAAC + LSKL ($n = 4$). Data are expressed as the mean ± SEM. *$P < 0.001$ DAAC + LSKL versus sham + saline. The difference between Sham + saline and Sham + LSKL is not statistically significant ($P < 0.09$) by Mann-Whitney analysis.

blasts, as well as in vascular endothelial and smooth muscle cells (data not shown). To confirm these immunohistochemical analyses, extracts of left ventricular tissues were probed for total and phosphorylated Smad 2 by immunoblotting (Figure 4C). Total Smad 2 was comparable in all groups, whereas phosphorylated Smad 2 was increased in DAAC hearts compared with sham hearts. Although measurement of TGF-β activity in tissues by immunohistochemical methods can be problematic, and in some studies, smad phosphorylation by advanced glycation end products is independent of TGF-β, results from these combined approaches strongly indicate that TGF-β activity is increased in this disease model.[53]

LSKL Blocking Peptide Improves Cardiac Function in DAAC Rats

To determine whether TSP1 is a key mechanism for TGF-β activation and fibrogenic progression in this model, a peptide antagonist (LSKL) of TSP1-dependent TGF-β activation or a control peptide (LSAL) was administered to both sham and DAAC animals. Peptides were administered by intraperitoneal injection, given every other day, starting 6 weeks after aortic coarctation and continuing through week 12. Peptides were detected in the urine of diabetic animals by mass spectrometry 24 hours following intraperitoneal administration of peptides, suggesting that the peptides achieve a systemic distribution (see Supplemental Figure S1 at *http://ajp.amjpathol.org*).

Animals were evaluated for cardiac function and fibrosis of the heart. Treatment with both control and active peptides had no effect on blood glucose levels in either sham or DAAC animals (Table 1). Treatment of DAAC rats with LSKL or LSAL peptides had no effect on body weight, blood glucose levels, water intake, LV weight, or LVW/HW (heart weight) and HW/BW (body weight) ratios. This is consistent with studies using anti-TGF-β-neutralizing antibodies, which showed that blood glucose levels were not affected by blocking TGF-β.[19]

Cardiac function was assessed by echocardiographic measurements (Table 2). DAAC animals showed a slight, but not significant, change in posterior wall thickness compared with sham or to DAAC rats treated with LSKL (Table 2). The diameter of the left ventricle in diastole (LVEDD) and systole (LVESD) were significantly increased in DAAC rats ($P < 0.05$) compared with sham rats. These dimensions were decreased in DAAC rats treated with LSKL ($P < 0.05$) compared with DAAC rats treated with saline or LSAL control peptide. Left ventricular remodeling and function as evaluated by LVEDD/PW ratio and VCFr (rate-corrected velocity of circumferential shortening) were adversely affected ($P < 0.05$) in DAAC animals compared with sham animals. In contrast, DAAC rats treated with LSKL peptide showed an increase ($P < 0.05$) in left ventricular function. Treatment with the LSKL peptide, but not the control LSAL peptide, also reduced myocyte hypertrophy (Table 1).

It is of note that neither active nor control peptide affected left ventricular function, body or heart weight, or blood glucose of sham control animals, indicating that the effect of the LSKL peptide is specific to TGF-β regulation in the DAAC condition. These data suggest that treatment with the TSP1 antagonist peptide improves cardiac function in DAAC rats.

The LSKL-Blocking Peptide Decreases Cardiac and Perivascular Fibrosis in DAAC Animals

Treatment of DAAC animals with LSKL markedly suppressed collagen deposition in the interstitium of the myocardium as determined by picric acid-Sirius red staining (Figure 5). No differences in collagen deposition were observed in DAAC animals treated with either saline or the control peptide LSAL (Figure 5A). Collagen deposition in both the epi- and endocardium was reduced by LSKL treatment (Figure 2B). Perivascular collagen was also reduced in LSKL-treated animals (Figure 5B).

Consistent with the decrease in fibrosis indicated by picric acid-Sirius red staining, hydroxyproline levels in the left ventricle were significantly decreased in LSKL-treated DAAC animals to levels comparable with sham animals (Figure 2C). Hydroxyproline levels were unaffected in animals treated with LSAL peptide (Figure 2C). Peptides did not affect hydroxyproline content in hearts of sham animals.

The LSKL Blocking Peptide Decreases TGF-β Activity and Smad 2 Phosphorylation

The LSKL peptide has been shown to reduce TGF-β activity *in vitro* and *in vivo*.[31,35,38,40,54] Therefore, to establish that the reduction in fibrosis in LSKL-treated animals is due to a reduction in active TGF-β, TGF-β activity was assessed by immunohistochemistry using an antibody specific for the active form of TGF-β (antibody LC1-30).[47,48] Staining for active TGF-β was significantly decreased in the myocardium of DAAC animals treated with LSKL peptide, but not in DAAC animals treated with either saline or LSAL control

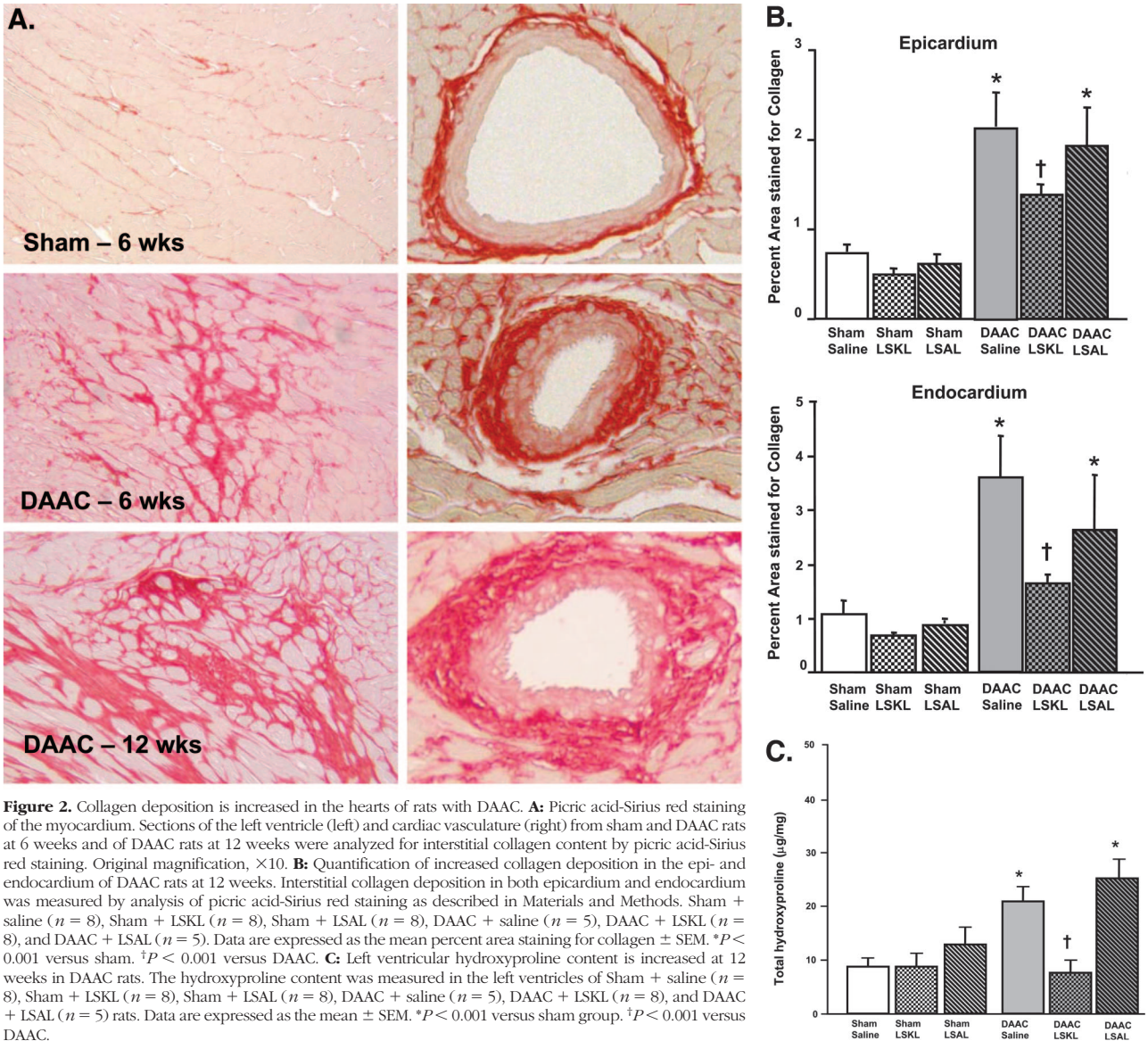

Figure 2. Collagen deposition is increased in the hearts of rats with DAAC. **A:** Picric acid-Sirius red staining of the myocardium. Sections of the left ventricle (left) and cardiac vasculature (right) from sham and DAAC rats at 6 weeks and of DAAC rats at 12 weeks were analyzed for interstitial collagen content by picric acid-Sirius red staining. Original magnification, ×10. **B:** Quantification of increased collagen deposition in the epi- and endocardium of DAAC rats at 12 weeks. Interstitial collagen deposition in both epicardium and endocardium was measured by analysis of picric acid-Sirius red staining as described in Materials and Methods. Sham + saline ($n = 8$), Sham + LSKL ($n = 8$), Sham + LSAL ($n = 8$), DAAC + saline ($n = 5$), DAAC + LSKL ($n = 8$), and DAAC + LSAL ($n = 5$). Data are expressed as the mean percent area staining for collagen ± SEM. $^{*}P < 0.001$ versus sham. $^{\dagger}P < 0.001$ versus DAAC. **C:** Left ventricular hydroxyproline content is increased at 12 weeks in DAAC rats. The hydroxyproline content was measured in the left ventricles of Sham + saline ($n = 8$), Sham + LSKL ($n = 8$), Sham + LSAL ($n = 8$), DAAC + saline ($n = 5$), DAAC + LSKL ($n = 8$), and DAAC + LSAL ($n = 5$) rats. Data are expressed as the mean ± SEM. $^{*}P < 0.001$ versus sham group. $^{\dagger}P < 0.001$ versus DAAC.

peptide (Figure 4A). Furthermore, LSKL peptide-treated animals showed a significant decrease in phosphorylated Smad2 in the heart compared with DAAC rats or DAAC animals treated with control (LSAL) peptide (Figure 4, B and C). LSKL reduced Smad 2 phosphorylation in the left ventricle to a level similar to sham animals, but it had no effect on Smad phosphorylation in the left ventricles of sham animals. Together, these data provide strong evidence that the LSKL peptide is acting to reduce TGF-β activity by preventing TSP1-dependent TGF-β activation.

Discussion

Fibrotic end-organ damage is a life-threatening consequence of hypertension and diabetes. Hypertension exacerbates myocardial complications associated with diabetes, resulting in more devastating structural and functional impairments than are caused by either disease.[1,2,55] The importance of fibrosis as a major determinant of myocardial performance and disease outcome is increasingly appreciated.

Despite the prevalence and the mortality associated with myocardial fibrosis, there are few effective therapies available that can either halt or reverse fibrotic organ damage. Antagonists of the renin-angiotensin system such as angiotensin-converting enzyme inhibitors and angiotensin receptor antagonists have been used to treat fibrotic complications of diabetes and hypertension.[1,15,56–60] Combined treatment with both an angiotensin-converting enzyme inhibitor and an AT1 receptor antagonist showed greater improvement of echocardiographic indices in type 2 diabetics than either therapy alone.[61] In addition, simultaneous blockade of Ang II and TGF-β reduces fibrotic disease considerably more than blockade of either agent alone, suggesting that additional factors contribute to myocardial dysfunction and fibrosis.[60] Following myocardial infarction, the incidence of heart failure and mortality rates are approximately twofold higher in patients with diabetes compared

with those without diabetes.[62] Despite the effectiveness of renin-angiotensin system antagonists, protection is not comparable with nondiabetic patients, and there can be cardiac side effects in a substantial number of patients.[63] Given that the presence of both pathologies greatly accelerates the development of cardiac failure, new strategies to prevent and treat cardiac complications in diabetic hypertensive patients are needed.

The major fibrogenic cytokine TGF-β is a potential therapeutic target, although a certain level of TGF-β activity is required for tissue homeostasis.[64,65] TGF-β activity is regulated at the level of protein expression and secretion, matrix deposition, and signaling.[23,26] However, a major point of control of TGF-β activity occurs at the level of its conversion from a latent complex to its biologically active form.[26] Previously, we identified the matrix glycoprotein TSP1 as the primary regulator of enhanced TGF-β activation due to glucose and/or angiotensin II by both rat mesangial cells and rat cardiac fibroblasts *in vitro*.[38] TGF-β activity under normal glucose conditions is unaffected by blocking TSP1-dependent TGF-β activation, whereas inhibition of TSP1 action completely blocks TGF-β activity stimulated by high concentrations of glucose, angiotensin II, or both agents in combination.[38]

In the current study, we used a rat model of diabetes and aortic abdominal coarctation to investigate the role of TSP1-dependent TGF-β activation in regulation of the excessive TGF-β activity and fibrosis in this disease. Rats are relatively resistant to atherosclerosis, and thus, alterations in cardiac function following streptozotocin treatment are believed to be due to cardiomyopathy and independent of atherosclerotic complications.[66] Hence, this is comparable with human diabetic cardiomyopathy. In this DAAC model, collagen accumulation, TSP1 expression, and TGF-β activity were all increased. There is also significant evidence of adverse left ventricular remodeling and systolic dysfunction.

Our finding that TSP1 is up-regulated is consistent with a recent report showing increased TSP1 immunostaining in the myocardium and small blood vessels in rats 4 weeks after STZ treatment.[36] The mechanism of the increase of TSP1 expression in the heart in these animals has not been established *in vivo*. Although TGF-β is a known regulator of TSP1 expression, especially in fibrotic kidney,[67–70] it seems that TGF-β itself is not a major regulator of TSP1 expression in this rat model of diabetes with abdominal aortic coarctation. TSP1 levels in myocar-

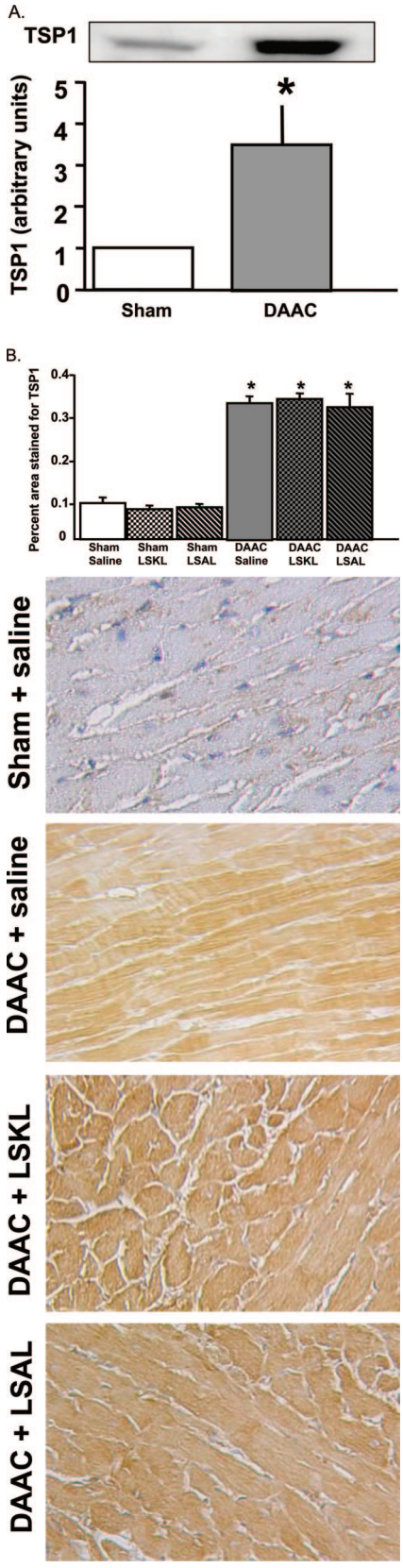

Figure 3. TSP1 is increased in the hearts of DAAC rats. **A:** Immunoblot of TSP1 in extracts of left ventricle at 12 weeks. Equal amounts of protein extracted from the left ventricles of sham and experimental animals were separated by sodium dodecyl sulfate-polyacrylamide gel electrophoresis (6% gel), transferred to polyvinylidene difluoride membranes, and immunoblotted with antibody to TSP1 and developed by enhanced chemiluminescence. The bands were quantified by densitometry ($n = 4$). Data are expressed as the mean ± SEM. $^*P < 0.001$ versus sham. **B:** Immunohistochemical staining for TSP1 in left ventricle. Sections were reacted with antibody specific for TSP1, color developed with diaminobenzidine, and counterstained with hematoxylin. The TSP1 immunostaining was quantified by morphometric analysis of 15 to 20 fields in each of three different regions of the left ventricle as described in Materials and Methods. Original magnification, ×20. Sham + saline ($n = 8$), Sham + LSKL ($n = 8$), Sham + LSAL ($n = 8$), DAAC + saline ($n = 5$), DAAC + LSKL ($n = 8$), and DAAC + LSAL ($n = 5$). Data are expressed as the mean percent area staining for TSP1 ± SEM. $^*P < 0.001$ versus sham.

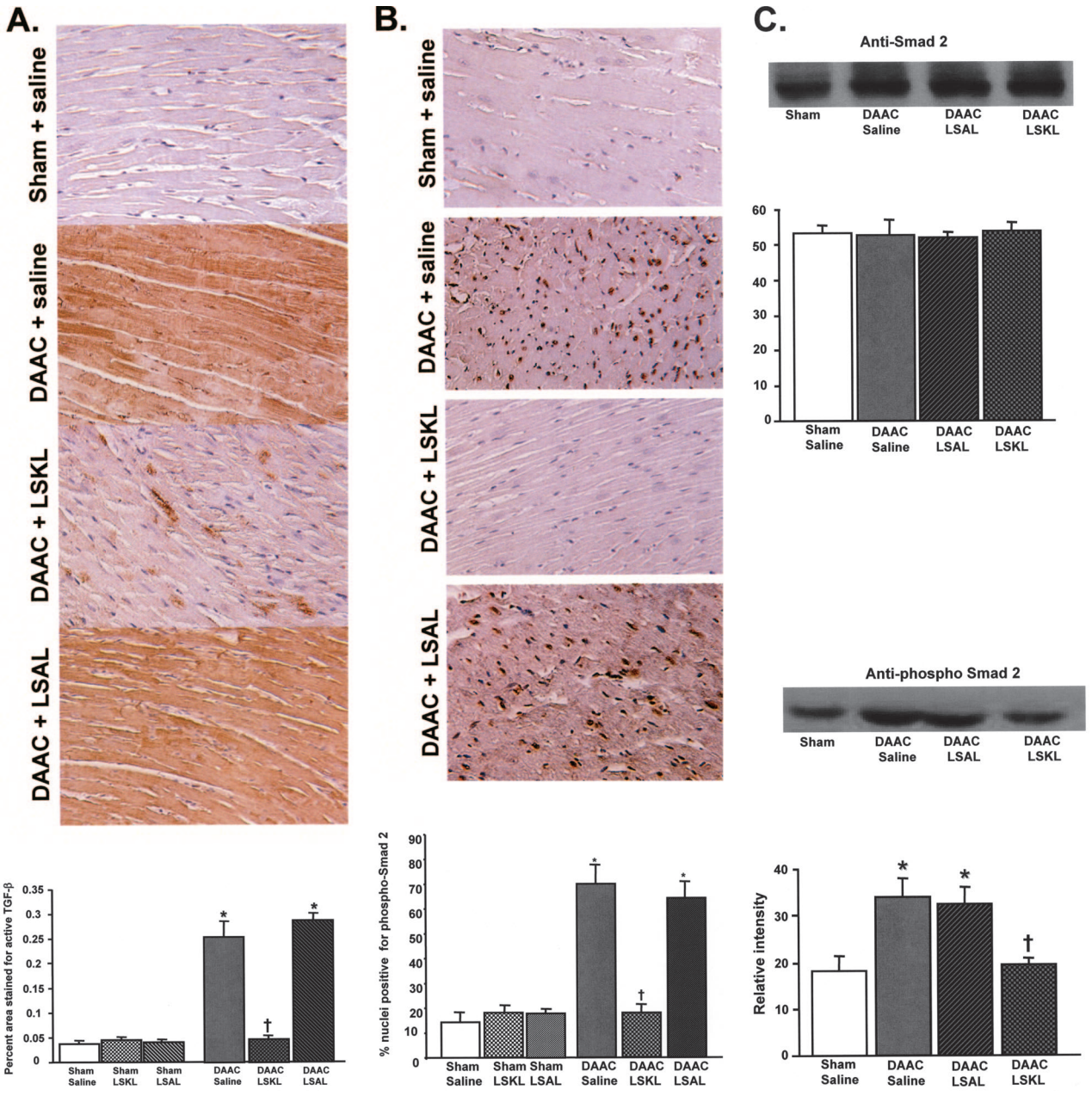

Figure 4. TGF-β signaling is increased in hearts of DAAC rats. **A:** Immunohistochemical staining for active TGF-β in the left ventricle 12 weeks after disease induction. Three different regions of the left ventricle were analyzed, and 10 to 15 fields were examined in each region. Sections were reacted with antibody specific for active TGF-β, color-developed with diaminobenzidine, and counterstained with hematoxylin. The percent area stained for active TGF-β was quantified as described in Materials and Methods. Original magnification, ×20. Sham + saline ($n = 8$), Sham + LSKL ($n = 8$), Sham + LSAL ($n = 8$), DAAC + saline ($n = 5$), DAAC + LSKL ($n = 8$), and DAAC + LSAL ($n = 5$). **B:** Immunohistochemical staining for nuclear phosphorylated Smad 2 in the left ventricle at 12 weeks. Tissue sections of the left ventricles were immunostained for phosphorylated Smad2, and the percentage of total nuclei stained positive (brown staining) was determined as described in Materials and Methods. Ten to 15 fields were examined in each region, and 80 to 128 nuclei were counted per field. Original magnification, ×20. Sham + saline ($n = 8$), Sham + LSKL ($n = 8$), Sham + LSAL ($n = 8$), DAAC + saline ($n = 5$), DAAC + LSKL ($n = 8$), and DAAC + LSAL ($n = 5$). Data are expressed as mean ± SEM. $^{*}P < 0.001$ versus sham. $^{\dagger}P < 0.001$ versus DAAC. **C:** Immunoblot for total and phosphorylated Smad 2 in extracts of the left ventricle at 12 weeks. Equal amounts of protein extracted from the left ventricles of sham and experimental animals were separated by sodium dodecyl sulfate-polyacrylamide gel electrophoresis (10% gels), transferred to polyvinylidene difluoride membranes, and immunoblotted separately with antibodies to phosphorylated Smad 2 (phospho-Smad2) or to Smad 2 (Smad2) and developed by enhanced chemiluminescence. The bands were quantified by densitometry ($n = 4$).

dial extracts were unchanged by LSKL peptide treatment in diabetic rats with renin-angiotensin activation. These observations are consistent with data from *in vitro* studies of rat mesangial cells, which showed that glucose stimulates increased TSP1 transcription through enhancing USF2-dependent transcription via protein kinase C, extracellular signal-regulated kinase, and p38 MAPK pathways to overcome nitric oxide-protein kinase G-mediated transcriptional repression.[41] The blocking peptide LSKL had no effect in these *in vitro* studies, suggesting that under high-glucose conditions, TGF-β is not a major regulator of TSP1.

Angiotensin II also up-regulates TSP1 in cardiac fibroblasts, endothelial cells, and mesangial cells through AT_1

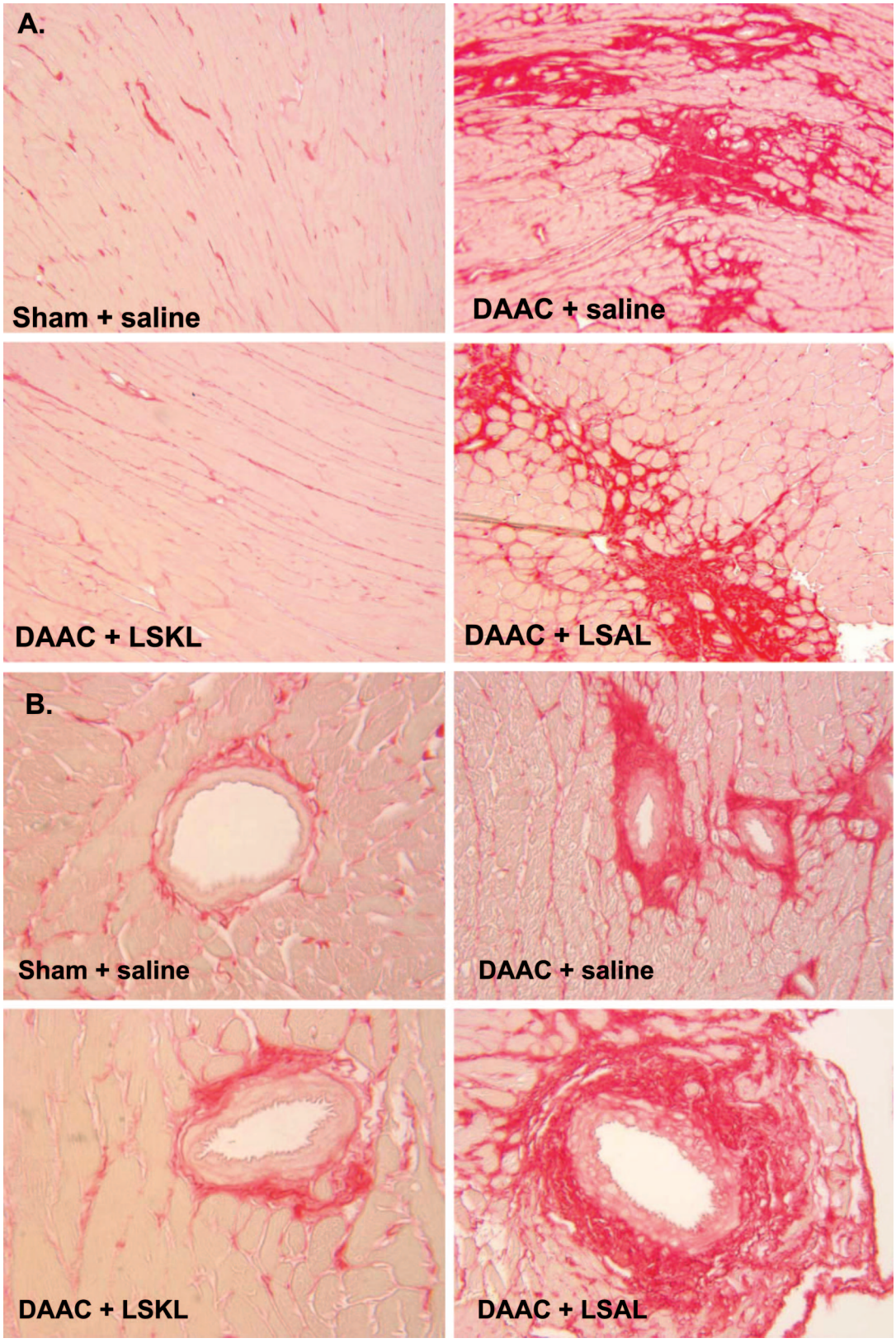

Figure 5. LSKL peptide treatment reduces fibrosis in hearts of DAAC rats. Sections of left ventricular myocardium (**A**) or vasculature (**B**) from DAAC rats after 12 weeks of disease induction and 6 weeks of treatment with saline, LSKL, or LSAL peptide were analyzed for interstitial collagen content by picric acid-Sirius red staining. Original magnification, ×10.

receptors.[38,39,71,72] TSP1 up-regulation by angiotensin II in mesangial cells occurs via AT_1 receptor signaling through the p38 MAPK and c-Jun NH_2-terminal kinase pathways.[39] Levels of TSP1 produced by combined stimulation with glucose and angiotensin II suggest that the pathways regulating TSP1 expression are likely parallel.[38] Thus in this DAAC model of myocardial fibrosis, it is likely that both glucose and angiotensin II are acting to stimulate TSP1 expression and consequent TGF-β activation. The involvement of the TSP1-TGF-β axis in other diseases in which myocardial fibrosis is an endpoint would probably depend on whether the pathogenic stimuli also increase TSP1 expression.

Blockade of TSP1-dependent activation of TGF-β by a peptide antagonist not only suppresses the development of cardiac fibrosis but also improves left ventricular function and cardiomyocyte hypertrophy. LSKL treatment improved LVEDD, LVEDD/PW, LVESD, and VCFr, indicating that the peptide antagonist prevented adverse left ventricular remodeling and left ventricular systolic dysfunction because of replacement fibrosis and myocyte dropout. Interestingly, normalization of left ventricular function and the reduction in fibrosis and myocyte hypertrophy by LSKL treatment occurred in the absence of changes in LV weight or the LV weight/HW ratio.

The TSP1 peptide antagonist attenuates fibrogenesis through prevention of TGF-β activation as measured by phosphorylated Smad 2 levels and immunostaining for active TGF-β levels in tissues. This peptide antagonist had no effect on normal blood glucose levels, blood pressure, or parameters of left ventricular function in sham control animals, suggesting that the peptide is indeed acting at the level of TGF-β regulation, specifically in response to the pathogenic stimuli of hyperglycemia and angiotensin II.

There are numerous therapeutic strategies under development aimed at targeting TGF-β, its receptors, signaling intermediates, downstream effectors, and endogenous inhibitors for potential use in the treatment of various types of fibrotic diseases.[14,73] Consistent with data from our previous *in vitro* studies, in the DAAC model the TSP1 antagonist peptide reduced only the excessive, stimulated levels of TGF-β activity and had no effects on basal levels of activity as measured in immunoblots for phosphorylated Smad 2. Because TGF-β activity is required for tissue homeostasis,[64,65] the ability to selectively target the pathological excess of TGF-β activity, without abrogating normal homeostatic levels of activity, represents an important therapeutic advantage for any antifibrotic approach that targets TGF-β. Genetic ablation of TGF-β, its receptors, or components of the Smad signaling pathway has serious consequences, including developmental defects, systemic inflammation, and increased tumorigenesis.[74–76] Although a number of different antagonists are being evaluated for clinical use, their spectrum of side effects remains unclear. Information regarding compromise of homeostatic functions of TGF-β from animal models or clinical trials with global TGF-β antagonists is limited.[73,77,78] In one systematic study performed in mice with life-long mammary-specific expression of a soluble TGF-β receptor antagonist, there were no significant differences in immune cell profiles or incidence of neoplasia, except for a slight increase in the CD4 and CD8 memory T-cell populations.[78] Although the long-term consequences of inhibiting TSP1-dependent TGF-β activation remain to be determined, in the present studies, systemic administration of the peptide over 6 weeks did not result in increased inflammation. Despite the lack of any obvious pathology in these present studies, further studies are being directed at determining whether inhibition of TSP1-dependent TGF-β activation exacerbates the impaired diabetic wound healing or alters immune cell profiles.

This work establishes the importance of TSP1 in regulating TGF-β activity diabetic and hypertensive fibrotic complications and demonstrates the potential for therapeutics targeted at blocking TGF-β activation for treatment of fibrotic complications because of angiotensin II and diabetes. It is worth noting that this work suggests that selective targeting of only pathological levels of TGF-β activity and maintenance of homeostatic levels of TGF-β might avoid the negative effects of more nonselective inhibition of TGF-β activity, such as inflammation and carcinogenesis.

Acknowledgments

We thank Wayne E. Bradley for excellent technical assistance, Mingli Liu for excellent animal care, and Dr. Dale Fowler for evaluation of TSP1 staining. We thank Dr. Kathleen Flanders, National Institutes of Health, for the generous gift of the anti-TGF-β antibody (LC-1-30), and Mr. Ray Moore of the University of Alabama Birmingham Mass Spectrometry facility for assistance with detection of the LSKL peptide.

References

1. Fonarow GC, Srikanthan P: Diabetic cardiomyopathy. Endocrinol Metab Clin North Am 2006, 35:575–599, ix
2. Asbun J, Villarreal FJ: The pathogenesis of myocardial fibrosis in the setting of diabetic cardiomyopathy. J Am Coll Cardiol 2006, 47:693–700
3. Factor SM, Bhan R, Minase T, Wolinsky H, Sonnenblick EH: Hypertensive-diabetic cardiomyopathy in the rat: an experimental model of human disease. Am J Pathol 1981, 102:219–228
4. Poornima IG, Parikh P, Shannon RP: Diabetic cardiomyopathy: the search for a unifying hypothesis. Circ Res 2006, 98:596–605
5. Factor SM, Minase T, Bhan R, Wolinsky H, Sonnenblick EH: Hypertensive diabetic cardiomyopathy in the rat: ultrastructural features. Virchows Arch A Pathol Anat Histopathol 1983, 398:305–317
6. Burlew BS, Weber KT: Cardiac fibrosis as a cause of diastolic dysfunction. Herz 2002, 27:92–98
7. Sadoshima J, Izumo S: Molecular characterization of angiotensin II–induced hypertrophy of cardiac myocytes and hyperplasia of cardiac fibroblasts. Critical role of the AT1 receptor subtype. Circ Res 1993, 73:413–423
8. Lim H, Zhu YZ: Role of transforming growth factor-β in the progression of heart failure. Cell Mol Life Sci 2006, 63:2584–2596
9. Rosenkranz S: TGF-β1 and angiotensin networking in cardiac remodeling. Cardiovasc Res 2004, 63:423–432
10. Asbun J, Manso AM, Villarreal FJ: Profibrotic influence of high glucose concentration on cardiac fibroblast functions: effects of losartan and vitamin E. Am J Physiol 2005, 288:H227–H234
11. Schultz Jel J, Witt SA, Glascock BJ, Nieman ML, Reiser PJ, Nix SL, Kimball TR, Doetschman T: TGF-β1 mediates the hypertrophic car-

diomyocyte growth induced by angiotensin II. J Clin Invest 2002, 109:787–796
12. Bujak M, Frangogiannis NG: The role of TGF-β signaling in myocardial infarction and cardiac remodeling. Cardiovasc Res 2007, 74:184–195
13. Zhong M, Zhang Y, Miao Y, Li L, Gong HP, Ma X, Sun H, Zhang W: [Mechanism of reversion of myocardial interstitial fibrosis in diabetic cardiomyopathy by valsartan]. Chinese. Zhonghua Yi Xue Za Zhi 2006, 86:232–236
14. Khan R: Examining potential therapies targeting myocardial fibrosis through the inhibition of transforming growth factor-β1. Cardiology 2007, 108:368–380
15. Jandeleit-Dahm K, Cooper ME: Hypertension and diabetes: role of the renin-angiotensin system. Endocrinol Metab Clin North Am 2006, 35:469–490, vii
16. Campbell SE, Katwa LC: Angiotensin II stimulated expression of transforming growth factor-β1 in cardiac fibroblasts and myofibroblasts. J Mol Cell Cardiol 1997, 29:1947–1958
17. Lijnen PJ, Petrov VV, Fagard RH: Induction of cardiac fibrosis by angiotensin II. Methods Find Exp Clin Pharmacol 2000, 22:709–723
18. Lijnen PJ, Petrov VV, Fagard RH: Induction of cardiac fibrosis by transforming growth factor-β_1. Mol Genet Metab 2000, 71:418–435
19. Sharma K, Jin Y, Guo J, Ziyadeh FN: Neutralization of TGF-β by anti-TGF-β antibody attenuates kidney hypertrophy and the enhanced extracellular matrix gene expression in STZ-induced diabetic mice. Diabetes 1996, 45:522–530
20. Kuwahara F, Kai H, Tokuda K, Kai M, Takeshita A, Egashira K, Imaizumi T: Transforming growth factor-β function blocking prevents myocardial fibrosis and diastolic dysfunction in pressure-overloaded rats. Circulation 2002, 106:130–135
21. Martin J, Kelly DJ, Mifsud SA, Zhang Y, Cox AJ, See F, Krum H, Wilkinson-Berka J, Gilbert RE: Tranilast attenuates cardiac matrix deposition in experimental diabetes: role of transforming growth factor-β. Cardiovasc Res 2005, 65:694–701
22. Habashi JP, Judge DP, Holm TM, Cohn RD, Loeys BL, Cooper TK, Myers L, Klein EC, Liu G, Calvi C, Podowski M, Neptune ER, Halushka MK, Bedja D, Gabrielson K, Rifkin DB, Carta L, Ramirez F, Huso DL, Dietz HC: Losartan, an AT1 antagonist, prevents aortic aneurysm in a mouse model of Marfan syndrome. Science 2006, 312:117–121
23. Massagué J, Wotton D: Transcriptional control by the TGF-β/Smad signaling system. EMBO J 2000, 19:1745–1754
24. Leask A, Abraham DJ: TGF-β signaling and the fibrotic response. FASEB J 2004, 18:816–827
25. Murphy-Ullrich JE, Poczatek M: Activation of latent TGF-β by thrombospondin-1: mechanisms and physiology. Cytokine Growth Factor Rev 2000, 11:59–69
26. Annes JP, Munger JS, Rifkin DB: Making sense of latent TGFβ activation. J Cell Sci 2003, 116:217–224
27. Barcellos-Hoff MH, Dix TA: Redox-mediated activation of latent transforming growth factor-β1. Mol Endocrinol 1996, 10:1077–1083
28. Munger JS, Huang X, Kawakatsu H, Griffiths MJ, Dalton SL, Wu J, Pittet JF, Kaminski N, Garat C, Matthay MA, Rifkin DB, Sheppard D: The integrin αvβ6 binds and activates latent TGFβ1: a mechanism for regulating pulmonary inflammation and fibrosis. Cell 1999, 96:319–328
29. Cambier S, Gline S, Mu D, Collins R, Araya J, Dolganov G, Einheber S, Boudreau N, Nishimura SL: Integrin $\alpha_v\beta$8-mediated activation of transforming growth factor-β by perivascular astrocytes: an angiogenic control switch. Am J Pathol 2005, 166:1883–1894
30. Schultz-Cherry S, Murphy-Ullrich JE: Thrombospondin causes activation of latent transforming growth factor-β secreted by endothelial cells by a novel mechanism. J Cell Biol 1993, 122:923–932
31. Ribeiro SM, Poczatek M, Schultz-Cherry S, Villain M, Murphy-Ullrich JE: The activation sequence of thrombospondin-1 interacts with the latency-associated peptide to regulate activation of latent transforming growth factor-beta. J Biol Chem 1999, 274:13586–13593
32. Young GD, Murphy-Ullrich JE: Molecular interactions that confer latency to transforming growth factor-β. J Biol Chem 2004, 279:38032–38039
33. Young GD, Murphy-Ullrich JE: The tryptophan-rich motifs of the thrombospondin type 1 repeats bind VLAL motifs in the latent transforming growth factor-β complex. J Biol Chem 2004, 279:47633–47642
34. Schultz-Cherry S, Chen H, Mosher DF, Misenheimer TM, Krutzsch HC, Roberts DD, Murphy-Ullrich JE: Regulation of transforming growth factor-β activation by discrete sequences of thrombospondin 1. J Biol Chem 1995, 270:7304–7310
35. Crawford SE, Stellmach V, Murphy-Ullrich JE, Ribeiro SM, Lawler J, Hynes RO, Boivin GP, Bouck N: Thrombospondin-1 is a major activator of TGF-β1 in vivo. Cell 1998, 93:1159–1170
36. Zhang XM, Shen F, Xv ZY, Yan ZY, Han S: Expression changes of thrombospondin-1 and neuropeptide Y in myocardium of STZ-induced rats. Int J Cardiol 2005, 105:192–197
37. Yevdokimova N, Wahab NA, Mason RM: Thrombospondin-1 is the key activator of TGF-β1 in human mesangial cells exposed to high glucose. J Am Soc Nephrol 2001, 12:703–712
38. Zhou Y, Poczatek MH, Berecek KH, Murphy-Ullrich JE: Thrombospondin 1 mediates angiotensin II induction of TGF-β activation by cardiac and renal cells under both high and low glucose conditions. Biochem Biophys Res Commun 2006, 339:633–641
39. Naito T, Masaki T, Nikolic-Paterson DJ, Tanji C, Yorioka N, Kohno N: Angiotensin II induces thrombospondin-1 production in human mesangial cells via p38 MAPK and JNK: a mechanism for activation of latent TGF-β1. Am J Physiol 2004, 286:F278–F287
40. Poczatek MH, Hugo C, Darley-Usmar V, Murphy-Ullrich JE: Glucose stimulation of transforming growth factor-β bioactivity in mesangial cells is mediated by thrombospondin-1. Am J Pathol 2000, 157:1353–1363
41. Wang S, Skorczewski J, Feng X, Mei L, Murphy-Ullrich JE: Glucose up-regulates thrombospondin 1 gene transcription and transforming growth factor-β activity through antagonism of cGMP-dependent protein kinase repression via upstream stimulatory factor 2. J Biol Chem 2004, 279:34311–34322
42. Borges GR, Oliveira M, Salgado HC, Fazan R Jr: Myocardial performance in conscious streptozotocin diabetic rats. Cardiovasc Diabetol 2006, 5:26
43. Schwarz ER, Pollick C, Meehan WP, Kloner RA: Evaluation of cardiac structures and function in small experimental animals: transthoracic, transesophageal, and intraventricular echocardiography to assess contractile function in rat heart. Basic Res Cardiol 1998, 93:477–486
44. Meng QC, Durand J, Chen YF, Oparil S: Simplified method for quantitation of angiotensin peptides in tissue. J Chromatogr 1993, 614:19–25
45. Wei CC, Tian B, Perry G, Meng QC, Chen YF, Oparil S, Dell'Italia LJ: Differential ANG II generation in plasma and tissue of mice with decreased expression of the ACE gene. Am J Physiol 2002, 282:H2254–H2258
46. Woessner Jr JE: The determination of hydroxyproline in tissue and protein samples containing small proportions of this imino acid. Arch Biochem Biophys 1961, 93:440–447
47. Flanders KC, Thompson NL, Cissel DS, Van Obberghen-Schilling E, Baker CC, Kass ME, Ellingsworth LR, Roberts AB, Sporn MB: Transforming growth factor-β1: histochemical localization with antibodies to different epitopes. J Cell Biol 1989, 108:653–660
48. Barcellos-Hoff MH, Ehrhart EJ, Kalia M, Jirtle R, Flanders K, Tsang ML: Immunohistochemical detection of active transforming growth factor-β in situ using engineered tissue. Am J Pathol 1995, 147:1228–1237
49. Hao J, Ju H, Zhao S, Junaid A, Scammell-La Fleur T, Dixon IM: Elevation of expression of Smads 2, 3, and 4, decorin and TGF-β in the chronic phase of myocardial infarct scar healing. J Mol Cell Cardiol 1999, 31:667–678
50. Weathington NM, van Houwelingen AH, Noerager BD, Jackson PL, Kraneveld AD, Galin FS, Folkerts G, Nijkamp FP, Blalock JE: A novel peptide CXCR ligand derived from extracellular matrix degradation during airway inflammation. Nat Med 2006, 12:317–323
51. Fernandes M, Onesti G, Weder A, Dykyj R, Gould AB, Kim KE, Swartz C: Experimental model of severe renal hypertension. J Lab Clin Med 1976, 87:561–567
52. Van Zwieten PA, Kam KL, Pijl AJ, Hendriks MG, Beenen OH, Pfaffendorf M: Hypertensive diabetic rats in pharmacological studies. Pharmacol Res 1996, 33:95–105
53. Li JH, Huang XR, Zhu HJ, Oldfield M, Cooper M, Truong LD, Johnson RJ, Lan HY: Advanced glycation end products activate Smad signaling via TGF-β-dependent and independent mechanisms: implications for diabetic renal and vascular disease. FASEB J 2004, 18:176–178
54. Daniel C, Wiede J, Krutzsch HC, Ribeiro SM, Roberts DD, Murphy-Ullrich JE, Hugo C: Thrombospondin-1 is a major activator of TGF-β in fibrotic renal disease in the rat in vivo. Kidney Int 2004, 65:459–468
55. Sowers JR, Epstein M, Frohlich ED: Diabetes, hypertension, and cardiovascular disease: an update. Hypertension 2001, 37:1053–1059

56. Zhu YC, Zhu YZ, Gohlke P, Stauss HM, Unger T: Effects of angiotensin-converting enzyme inhibition and angiotensin II AT1 receptor antagonism on cardiac parameters in left ventricular hypertrophy. Am J Cardiol 1997, 80:110A–117A
57. Cooper ME: The role of the renin-angiotensin-aldosterone system in diabetes and its vascular complications. Am J Hypertens 2004, 17: 16S–20S; quiz A12–A14
58. Cooper ME, Tikellis C, Thomas MC: Preventing diabetes in patients with hypertension: one more reason to block the renin-angiotensin system. J Hypertens 2006, 24(Suppl):S57–S63
59. Lim HS, MacFadyen RJ, Lip GY: Diabetes mellitus, the renin-angiotensin-aldosterone system, and the heart. Arch Intern Med 2004, 164:1737–1748
60. Yu L, Border WA, Anderson I, McCourt M, Huang Y, Noble NA: Combining TGF-beta inhibition and angiotensin II blockade results in enhanced antifibrotic effect. Kidney Int 2004, 66:1774–1784
61. Symeonides P, Koulouris S, Vratsista E, Triantafyllou K, Ioannidis G, Thalassinos N, Katritsis D: Both ramipril and telmisartan reverse indices of early diabetic cardiomyopathy: A comparative study. Eur J Echocardiogr 2006, [Epub ahead of print]
62. Solomon SD, St. John Sutton M, Lamas GA, Plappert T, Rouleau JL, Skali H, Moye L, Braunwald E, Pfeffer MA: Ventricular remodeling does not accompany the development of heart failure in diabetic patients after myocardial infarction. Circulation 2002, 106:1251–1255
63. Grossman E, Messerli FH: Long-term safety of antihypertensive therapy. Prog Cardiovasc Dis 2006, 49:16–25
64. Boivin GP, O'Toole BA, Orsmby IE, Diebold RJ, Eis MJ, Doetschman T, Kier AB: Onset and progression of pathological lesions in transforming growth factor-β1-deficient mice. Am J Pathol 1995, 146:276–288
65. Bommireddy R, Saxena V, Ormsby I, Yin M, Boivin GP, Babcock GF, Singh RR, Doetschman T: TGF-β1 regulates lymphocyte homeostasis by preventing activation and subsequent apoptosis of peripheral lymphocytes. J Immunol 2003, 170:4612–4622
66. Tomlinson KC, Gardiner SM, Hebden RA, Bennett T: Functional consequences of streptozotocin-induced diabetes mellitus, with particular reference to the cardiovascular system. Pharmacol Rev 1992, 44:103–150
67. Tada H, Kuboki K, Nomura K, Inokuchi T: High glucose levels enhance TGF-β1-thrombospondin-1 pathway in cultured human mesangial cells via mechanisms dependent on glucose-induced PKC activation. J Diabetes Complications 2001, 15:193–197
68. Nakagawa T, Li JH, Garcia G, Mu W, Piek E, Bottinger EP, Chen Y, Zhu HJ, Kang DH, Schreiner GF, Lan HY, Johnson RJ: TGF-β induces proangiogenic and antiangiogenic factors via parallel but distinct Smad pathways. Kidney Int 2004, 66:605–613
69. Nakagawa T, Lan HY, Glushakova O, Zhu HJ, Kang DH, Schreiner GF, Bottinger EP, Johnson RJ, Sautin YY: Role of ERK1/2 and p38 mitogen-activated protein kinases in the regulation of thrombospondin-1 by TGF-β1 in rat proximal tubular cells and mouse fibroblasts. J Am Soc Nephrol 2005, 16:899–904
70. Penttinen RP, Kobayashi S, Bornstein P: Transforming growth factor beta increases mRNA for matrix proteins both in the presence and in the absence of changes in mRNA stability. Proc Natl Acad Sci USA 1988, 85:1105–1108
71. Fischer JW, Stoll M, Hahn AW, Unger T: Differential regulation of thrombospondin-1 and fibronectin by angiotensin II receptor subtypes in cultured endothelial cells. Cardiovasc Res 2001, 51:784–791
72. Chua CC, Hamdy RC, Chua BH: Regulation of thrombospondin-1 production by angiotensin II in rat heart endothelial cells. Biochim Biophys Acta 1997, 1357:209–214
73. Denton CP, Merkel PA, Furst DE, Khanna D, Emery P, Hsu VM, Silliman N, Streisand J, Powell J, Akesson A, Coppock J, Hoogen F, Herrick A, Mayes MD, Veale D, Haas J, Ledbetter S, Korn JH, Black CM, Seibold JR: Recombinant human anti-transforming growth factor β1 antibody therapy in systemic sclerosis: a multicenter, randomized, placebo-controlled phase I/II trial of CAT-192. Arthritis Rheum 2007, 56:323–333
74. Letterio JJ, Bottinger EP: TGF-beta knockout and dominant-negative receptor transgenic mice. Miner Electrolyte Metab 1998, 24:161–167
75. Tian F, Byfield SD, Parks WT, Stuelten CH, Nemani D, Zhang YE, Roberts AB: Smad-binding defective mutant of transforming growth factor β type I receptor enhances tumorigenesis but suppresses metastasis of breast cancer cell lines. Cancer Res 2004, 64:4523–4530
76. Christ M, McCartney-Francis NL, Kulkarni AB, Ward JM, Mizel DE, Mackall CL, Gress RE, Hines KL, Tian H, Karlsson S: Immune dysregulation in TGF-β 1-deficient mice. J Immunol 1994, 153:1936–1946
77. Iyer S, Wang ZG, Akhtari M, Zhao W, Seth P: Targeting TGFβ signaling for cancer therapy. Cancer Biol Ther 2005, 4:261–266
78. Yang YA, Dukhanina O, Tang B, Mamura M, Letterio JJ, MacGregor J, Patel SC, Khozin S, Liu ZY, Green J, Anver MR, Merlino G, Wakefield LM: Lifetime exposure to a soluble TGF-β antagonist protects mice against metastasis without adverse side effects. J Clin Invest 2002, 109:1607–1615